



Deposited via The University of Leeds.

White Rose Research Online URL for this paper:

<https://eprints.whiterose.ac.uk/id/eprint/103772/>

Version: Accepted Version

Article:

Raza, G, Amjad, M, Kaur, I et al. (2016) Stability and Aggregation Kinetics of Titania Nanomaterials under Environmentally Realistic Conditions. *Environmental science & technology*, 50 (16). pp. 8462-8472. ISSN: 0013-936X

<https://doi.org/10.1021/acs.est.5b05746>

Reuse

Items deposited in White Rose Research Online are protected by copyright, with all rights reserved unless indicated otherwise. They may be downloaded and/or printed for private study, or other acts as permitted by national copyright laws. The publisher or other rights holders may allow further reproduction and re-use of the full text version. This is indicated by the licence information on the White Rose Research Online record for the item.

Takedown

If you consider content in White Rose Research Online to be in breach of UK law, please notify us by emailing eprints@whiterose.ac.uk including the URL of the record and the reason for the withdrawal request.

Stability and Aggregation Kinetics of Titania Nanomaterials under Environmentally Realistic Conditions

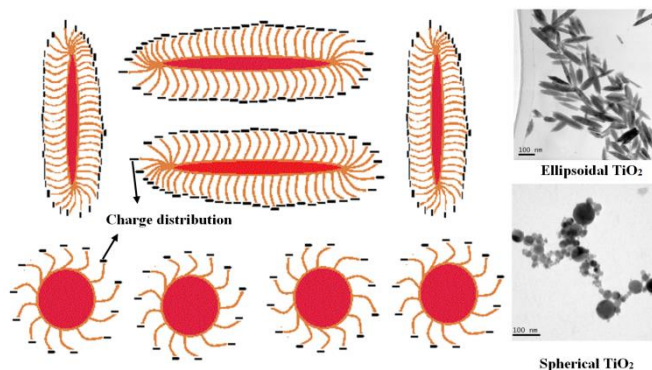
Ghulam Raza^{*†} Muhammad Amjad^{†, §} Inder Kaur[✧] Dongsheng Wen^{*†}

[†] School of Process, Environmental and Materials Engineering, University of Leeds, Leeds, LS2 9JU, UK

[✧] School of Geography, Earth and Environmental Sciences, University of Birmingham, Birmingham, UK

[§] Department of Mechanical Engineering, University of Engineering and Technology Lahore (City Campus), Pakistan

Abstract: Nanoparticle morphology is expected to play a significant role in the stability, aggregation behaviour and ultimate fate of engineered nanomaterials in natural aquatic environments. The aggregation kinetics of ellipsoidal and spherical titanium dioxide (TiO₂) nanoparticles (NP) under different



surfactant loadings, pH values and ionic strengths are investigated in this study. The stability results reveal that alteration of surface charge is the stability determining factor. Among five different surfactants investigated, sodium citrate and Suwannee river fulvic acid (SRFA) were the most effective stabilizers. It was observed that both types of NP were more stable in monovalent salts (NaCl and NaNO₃) as compared with divalent salts (Ca(NO₃)₂ and CaCl₂). The aggregation of spherical TiO₂ NP demonstrated a strong dependency on the ionic strength regardless of the presence of mono or divalent salts; while the ellipsoids exhibited a lower dependency on the ionic strength but is more stable. This work acts as a benchmark study towards understanding the fate of stabilized NP in natural environments that are rich in Ca(CO₃)₂, NaNO₃, NaCl and CaCl₂ along with natural organic matters.

Keywords: Nanoparticle, stability, aggregation, kinetics, surfactants, sticking efficiency

27 INTRODUCTION

28 TiO₂ is a multipurpose material widely used in nano-particulate form¹. TiO₂ nanoparticles (NP) are
29 routinely used in products like sun creams, cosmetics, paints, self-cleaning dispersions, textiles, sports
30 equipment, solar cells and waste water treatment devices². Its unique properties give it an increased
31 demand in different industries but at the same time causes increasing environmental concerns.

32 It is understood that the migration behaviour, toxicity and bioavailability of NP are governed by
33 their physico-chemical properties such as shape, size, surface area, agglomeration state, zeta potential
34 and surface chemistry^{3, 4}. In the past decade, the aggregation kinetics of different NP has been
35 extensively investigated⁵⁻¹⁰. As TiO₂ NP have the tendency to aggregate and coalesce into big
36 particles, which is undesirable for most of the applications¹¹, their colloidal stability investigation
37 becomes important^{12, 13}. Most of the physico-chemical properties of NP are related to their behaviours
38 in dispersions including the reactions at the particle–liquid interface¹⁴.

39 To fully evaluate the environmental implications, the mobility and risks of such NPs, the
40 knowledge regarding their interaction with different media constituents and the aggregation kinetics
41 are essential. Several factors are responsible for NP aggregation as studied by different scientists¹⁵⁻¹⁸.
42 Firstly, the surface charge of the NP greatly influence their solubility and hence the stability. Surface
43 charge results in either attractive (positive-negative interaction) or repulsive (similar charge
44 interactions) energies, which depend on the pH, temperature and the concentration and type of the
45 electrolyte in the medium. The presence of electrolytes in the medium would alter the stability and
46 agglomeration state of NP dispersions. Secondly, the concentration of the NP precursors, polymers,
47 surfactants and the temperature would alter the overall stability of dispersions. Water or other
48 molecules could interact with NP and alter their crystal structures. Zinc sulphide (ZnS) NP is a good
49 example as reported by Zhang et al. (2003), where 3 nm ZnS NP containing around 700 atoms
50 rearranged their crystal structures after the interaction with water to form more ordered bulk
51 structure¹⁹. Guzman and co-workers²⁰ showed a pHzpc (i.e., pH at point of zero charge) dependence
52 of titania NP while French et al.²¹ observed the influence of ionic strength (IS), on the aggregation

53 kinetics of 50-60 nm TiO₂ agglomerates (with 5 nm primary size) at low IS. Similarly surface charge
54 and zeta-potential has a strong correlation with the aggregation kinetics of ZnO NP²². In an interesting
55 study on the aggregation kinetics²³, Suwannee river fulvic acid (SRFA)-stabilized TiO₂ NP showed
56 strong stability at varying IS under acidic pH, while became aggregated under low IS at neutral pH
57 values.

58 It shall be noted that many reported aggregation kinetic studies were based on colloids made from
59 pre-fabricated nanomaterials²⁴⁻²⁷, which inevitably contained many agglomerated NP due to the
60 difficulty in dispersing them to their primary sizes. The aggregation kinetics, therefore, would be
61 different to those well-dispersed colloids. The aggregation kinetics of NP is controlled by the
62 electrostatic forces and the electrosteric interferences. The magnitude of the electrosteric interferences
63 depends on the concentration of the stabilizing agent, coating thickness, the conformation and
64 dimensions of the adsorbed double layer^{17, 28}. From the environmental concern, the fate of NP in an
65 aqueous system is dependent on both particle characteristics and the complex water chemistry such as
66 pH, ionic strength and dissolved organic matter contents and properties, which may stabilize or
67 agglomerate the NP influencing the transport of NP. Quite a few studies²⁹⁻³² have been conducted to
68 investigate the effect of these influential factors, but no solid conclusion was reached and the
69 understanding on the fate of NP under different environmental conditions is still very limited.
70 Although there were a few studies on the transport of TiO₂ NP with particular reference to ionic
71 strength and surfactants^{33, 34}, the influence of particle morphology is essentially lacking, hence the
72 effects of ionic strength and surfactants on the aggregation kinetics are in-conclusive.

73 This work aims to address these limitations by conducting a detailed study of the stability and
74 aggregation kinetics of stable TiO₂ NP and investigate the influence of particle morphology under
75 environmental-like conditions. For this purpose, two different shaped TiO₂ colloids, i.e. ellipsoids and
76 spherical NP, were synthesized. The aggregation kinetics of well-dispersed NP was assessed under
77 five different stabilizing agents and four different ionic strengths. From the practical consideration,

78 the aggregation kinetics study was conducted at neutral pH values. This detailed study shall advance
79 the understanding in the ultimate fate of TiO₂ NP in complex environmental conditions.

80 **MATERIALS AND METHODS**

81 **Materials preparation**

82 All surfactants except Suwannee river fulvic acid (SRFA) were purchased from Sigma Aldrich and
83 used without further purification. SRFA was purchased from International Humic Substances Society
84 (Atlanta, USA) while HCl and NaOH (0.01-0.1M) were purchased from Fisher Scientific for pH
85 adjustment. Two types of titania NP were selected from many batches of self-fabricated lots. The only
86 precursor used in this research, i.e. 99% pure TiCl₄, was purchased from Sigma Aldrich. Briefly TiO₂
87 NP were synthesized by a modified hydrothermal methodology, similar to the one reported by Yin et
88 al³⁵. In a typical synthesis, solution 1 was made by diluting TiCl₄ to 1mol/L with 5% HCl in an ice
89 bath. Solution 2 was prepared at different alcohol to water ratios (i.e., 1:2 Ethanol: Water, 1:2
90 Methanol: Water and 1:2 Acetone: Water). Both solutions 1 and 2 were mixed to get 0.1mol/L final
91 concentration of TiCl₄. Ice cooled temperature was maintained throughout the preparation process.
92 For rutile ellipsoids synthesis, the final dispersion was stirred for 30 minutes with magnetic stirrer at
93 45°C temperature while for spherical anatase NP, the dispersion was treated at a temperature of 110°C
94 for 40 minutes using Teflon lined vessels in a microwave oven (MARS 5). Finally three repetitive
95 washings with DI water and acetone were given to NP by centrifugation.

96 A 20 ml dispersion of 20 ppm spherical NP was stabilized with different surfactants including
97 polyethylene glycol (PEG), Polyvinylpyrrolidone (PVP), sodium dodecyl sulfate (SDS) and
98 Suwannee river fulvic acid (SRFA). The concentrations of all surfactants were optimized for spherical
99 NPs and similar concentrations were used for ellipsoids for all experiments. When stabilized in SRFA
100 and sodium citrate, rutile ellipsoids and anatase spherical NPs were tested for their aggregation
101 kinetics against different salt concentrations (NaCl, NaNO₃, Ca(NO₃)₂ and CaCl₂).

102 An advanced X-Ray diffraction spectroscopy (Bruker D-8, installed with PANalytical X'pert Pro
103 software), Transmission electron microscope (TEM, Tecnai F-20) and Malvern Zetasizer (NanoZS90
104 5001) were used for NP characterization. For TEM study, rutile ellipsoids and anatase spherical NP
105 were stabilized with 0.3% sodium citrate and SRFA100 (i.e., the concentration of SRFA is 100 ppm).
106 Holey carbon film TEM copper grids were purchased from Agar Scientific. In a typical preparation
107 process, the NP sample was diluted 100 times and a 10 μ l drop of the dilute was sandwiched between
108 two DI water drops of 50 μ l. The grid was dried in a clean environment under room temperature and
109 rinsed with DI water to remove any dirt or excessive materials. The grids for aggregation kinetics
110 were prepared without diluting the samples, by following the same grid preparation methodology.

111 **Time resolved aggregation kinetics**

112 Time-resolved DLS (Dynamic Light Scattering) measurements of aggregating TiO₂ NP were
113 performed at 20⁰C except for the zeta potential, which were done at 25⁰C as per Malvern instructions.
114 The scattering angle was 90⁰ for all measurements. The concentration of the fabricated nanoparticles
115 dispersion was measured by an atomic absorption spectrometer (AAS, Varian AA240FS) and a fixed
116 TiO₂ concentration of 20 ppm was used via dilution in all experiments. In the experiments, 1 ml of
117 nanoparticle dispersion was mixed with different amounts of mono or divalent dispersions in a mixing
118 vial to reach desired concentration of electrolytes. The resulting dispersion was shaken gently and
119 transferred quickly to DLS cuvettes for the measurement. Every reading was taken at 10 second
120 interval with the maximum of 500 readings. The effect of pH, surfactants and zeta potential on the
121 aggregation kinetics was studied for a period of 2 weeks.

122 The aggregation kinetics was derived from experimentally-measured particle size data. At the early
123 stage, the formation of doublets (i.e., usually considered at the time where the initial aggregate
124 hydrodynamic diameter increases by one quarter of its original size) was expressed in Eq.(1)³⁶

$$\left(\frac{\Delta a_h(t)}{\Delta t}\right)_{t \rightarrow 0} \propto k_{11} N_0 \quad (1)$$

125 where $a_h(t)$ is the aggregation size over time t , N_0 is the starting number concentration of NP
126 dispersion and k_{11} is the rate of formation of doublets. These doublets increase in number at a faster
127 rate with an increase in ion concentration in the dispersion due to the suppression of diffused double
128 layer (DDL). This suppression of DDL leads to a decrease in the van der Waal forces between
129 particles. At a point when all the van der Waal forces are overwhelmed, k_{11} becomes equal to the
130 diffusion limited aggregation rate, i.e., k_{slow} , which shows the overall aggregation rate. The
131 Smoluchowski aggregation rate, or k_{fast} , was calculated by Eq. (2)³⁷

$$k_{fast} = 8kT/3u \quad (2)$$

132 where k represents Boltzmann's constant, u is the liquid's viscosity and T is the temperature. The
133 sticking efficiency ' α ' is defined as the ratio of k_{slow} and k_{fast} , as in Eq.(3), which is the average of
134 the fastest points of aggregation stage at a specific ionic strength,

$$\alpha = \frac{k_{slow}}{k_{fast}} \quad (3)$$

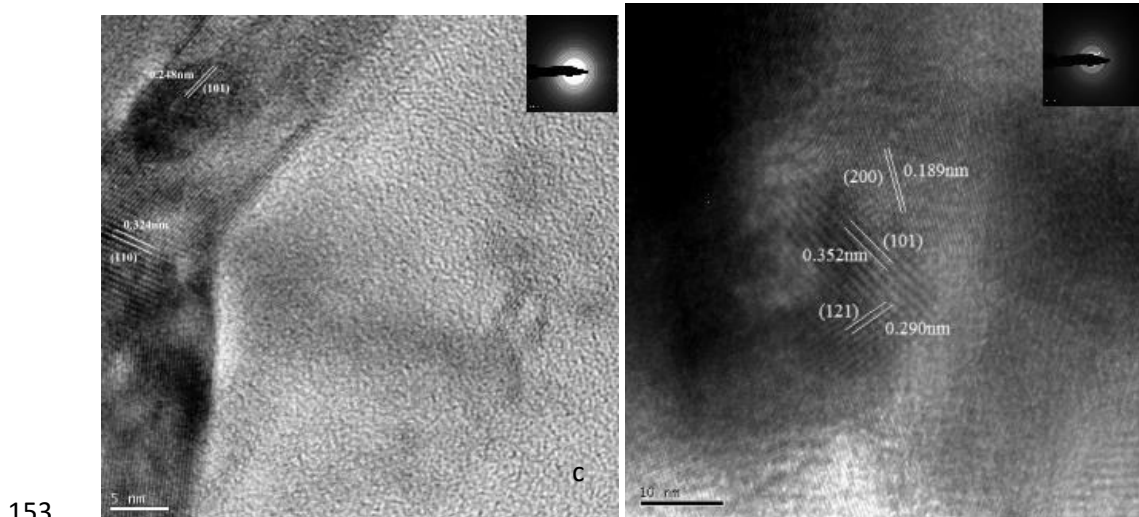
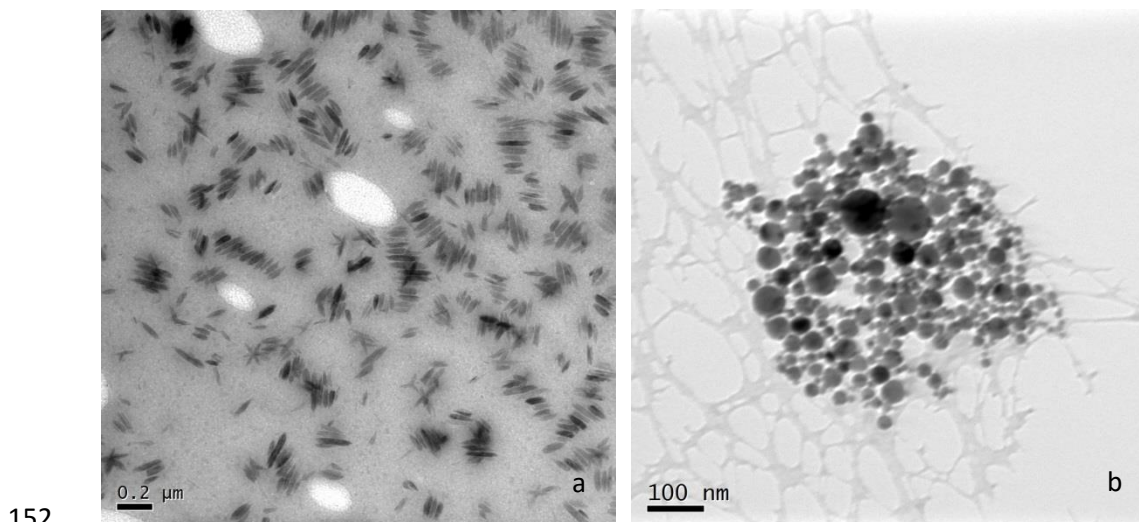
135 and the critical coagulation concentration (CCC) is the concentration value when α approaches to a
136 value of 1.

137 **RESULTS AND DISCUSSION**

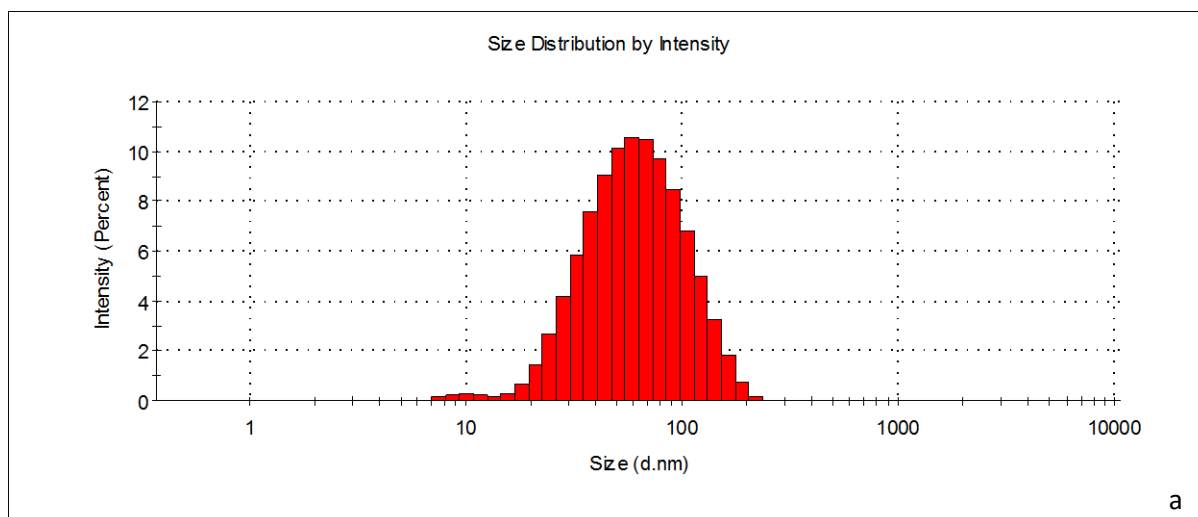
138 **TiO₂ characterization**

139 The average length of rutile ellipsoids measured by TEM was 100±20nm (i.e. from randomly
140 selected 214 ellipsoids) with average width of 20±5nm, which gives an aspect ratio of 4.5±0.3 and a
141 hydrodynamic diameter of 55±5. The ellipsoids used for stability experiments were dispersed for a
142 period over 6 months with no aggregation or agglomeration as measured by the DLS method. The
143 spherical NP had a core size range between 60±35nm³⁸ and hydrodynamic diameter of 100±10nm for
144 both citrate and SRFA100 stabilised. Figure 1a and 1b show TEM micrograph of SRFA stabilized
145 rutile ellipsoids and spherical anatase NP respectively, with detailed morphology shown by HRTEM
146 in Figure 1c and 1d. HRTEM micrograph of the rutile TiO₂ (Figure 1c) shows lattice fringes with d-

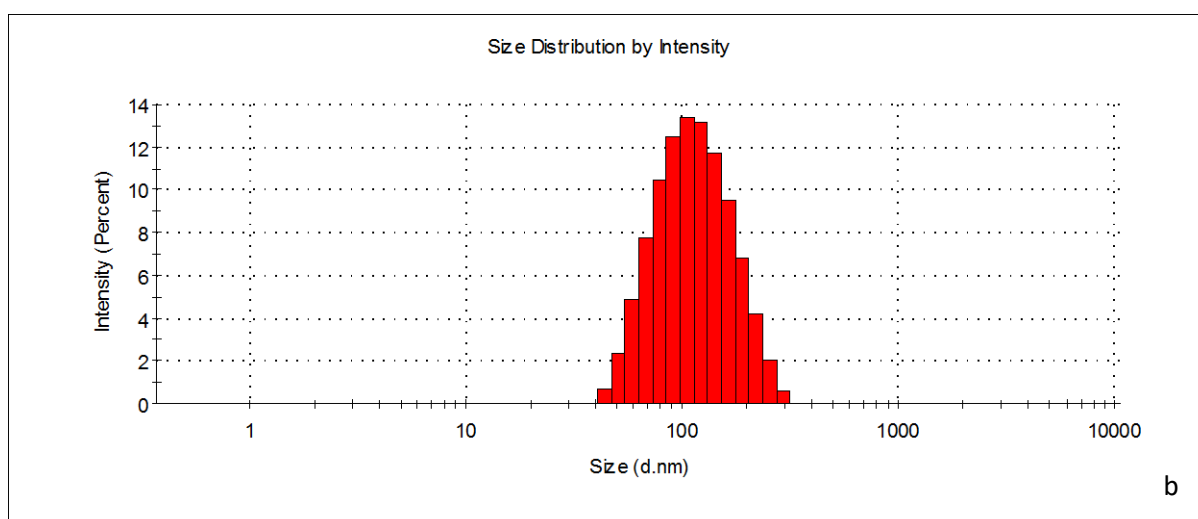
147 spacing of 0.248nm, corresponding to (101) plane, and 0.324nm, corresponding to (110) of the rutile
148 phase. HRTEM micrograph of the anatase TiO₂ (Figure 1d) shows lattice fringes with d-spacing of
149 0.189 nm, which corresponds to the (200) plane, 0.352nm corresponding to (101) plane and 0.290nm
150 (121) planes of the anatase phase. Figures 2a and 2b illustrate the hydrodynamic particle size
151 distribution of TiO₂ ellipsoids and spherical NP in water respectively.



154 Figure 1: a) TEM micrograph of TiO₂ ellipsoids dispersed with SRFA100; b) Spherical anatase NP
155 stabilized with SRFA100; c) HRTEM of TiO₂ ellipsoids with SAED pattern showing lattice fringes
156 (101) and (110); d) HRTEM of spherical anatase with SAED pattern showing lattice fringes (101),
157 (200) and (121)



158



159

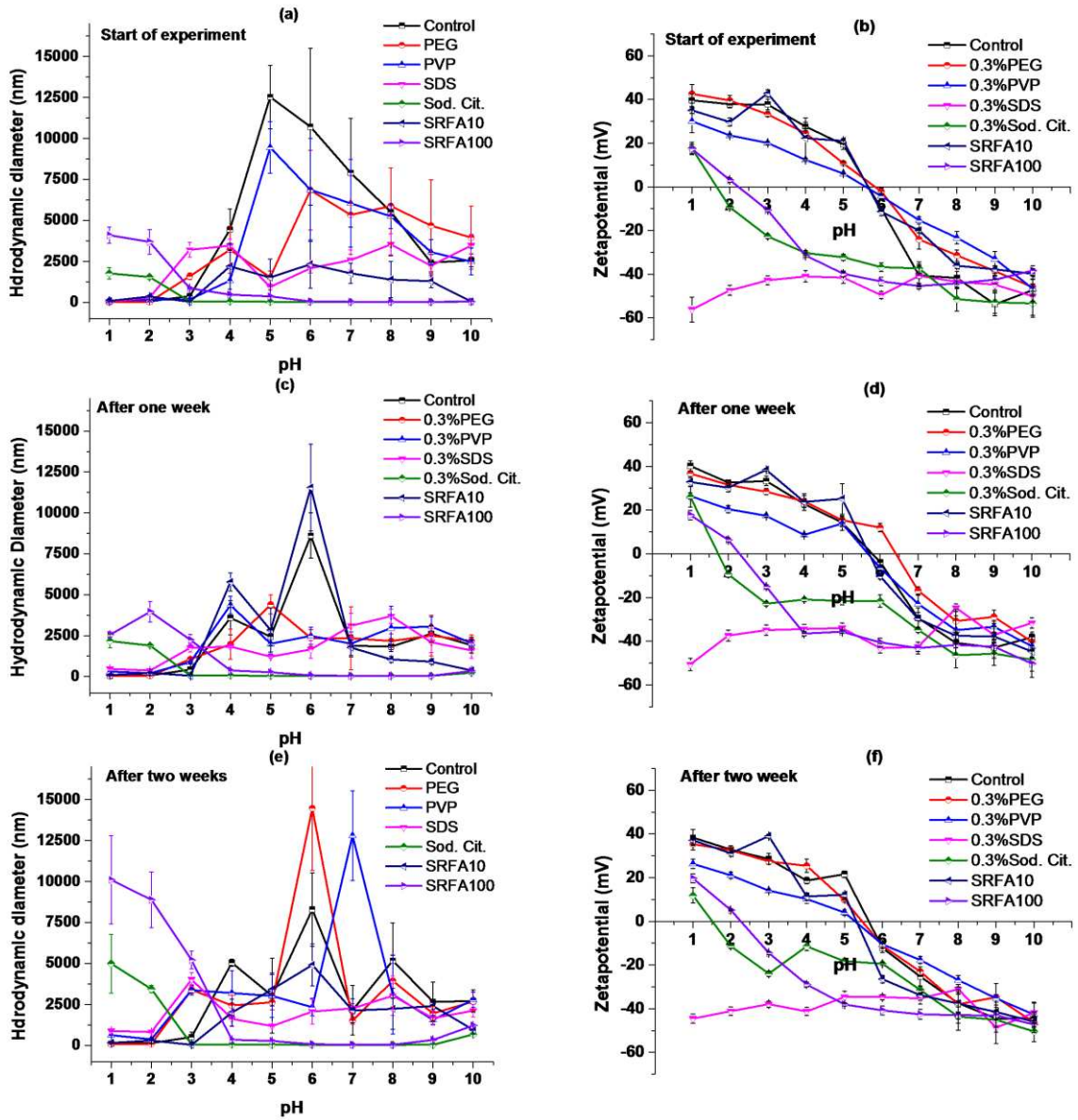
160 Figure 2: a) DLS histogram of TiO₂ ellipsoids dispersed with SRFA100 and b) DLS histogram of
 161 spherical anatase NP stabilized with SRFA100. (All measurements were taken at pH 6.5±0.2 without
 162 any electrolyte).

163 **Impact of surface functionalization on the stability of TiO₂**

164 Spherical anatase NPs were tested for their stability at different pH values in the presence of
 165 different surfactants. Results from different surfactants treatment revealed a change in size and zeta
 166 potential over a period of 2 weeks. The dispersion without surfactants was most unstable at all pH
 167 values except the highly acidic range (Figure 3a). Large agglomerates were observed at pH 5 which is
 168 near to the point of zero charge (pH_{zpc}), i.e. pH=5.6. Sodium citrate showed the greatest stabilization
 169 for almost all pH values except the highly acidic range (pH 1-3) because pH_{zpc} was shifted to these

170 values. No significant change was observed in the change of hydrodynamic size in pH 3-9 over the
171 period of two weeks. The standard deviations of change in hydrodynamic diameter for three replicates
172 show that there was inconsequential change, confirming the stability at a range of pH values. The
173 control, PEG and PVP stabilized dispersion showed high aggregation rate at a pH value near to the
174 point of zero charge (pH_{zpc}), as seen by the large aggregates near pH_{zpc} .

175 The point of zero charge for sodium citrate and SRFA was 1.6 and 2.3 respectively. The zeta
176 potential for 0.3% SDS remained on negative values from pH1 up to pH10. The size change was
177 fairly consistent with the positive and negative charge of the particles for all the surfactants over a
178 period of two weeks. Generally the presence of negative charge on particles contributes to stabilising
179 nanoparticles but this is not true with 0.3 mass percentage of SDS. This may be attributed to critical
180 micelle concentration (CMC) of SDS which is 8.2 mM (0.00082%) in water at 25°C and above
181 which micelles form and all additional surfactants added to the system go to micelles ³⁹.

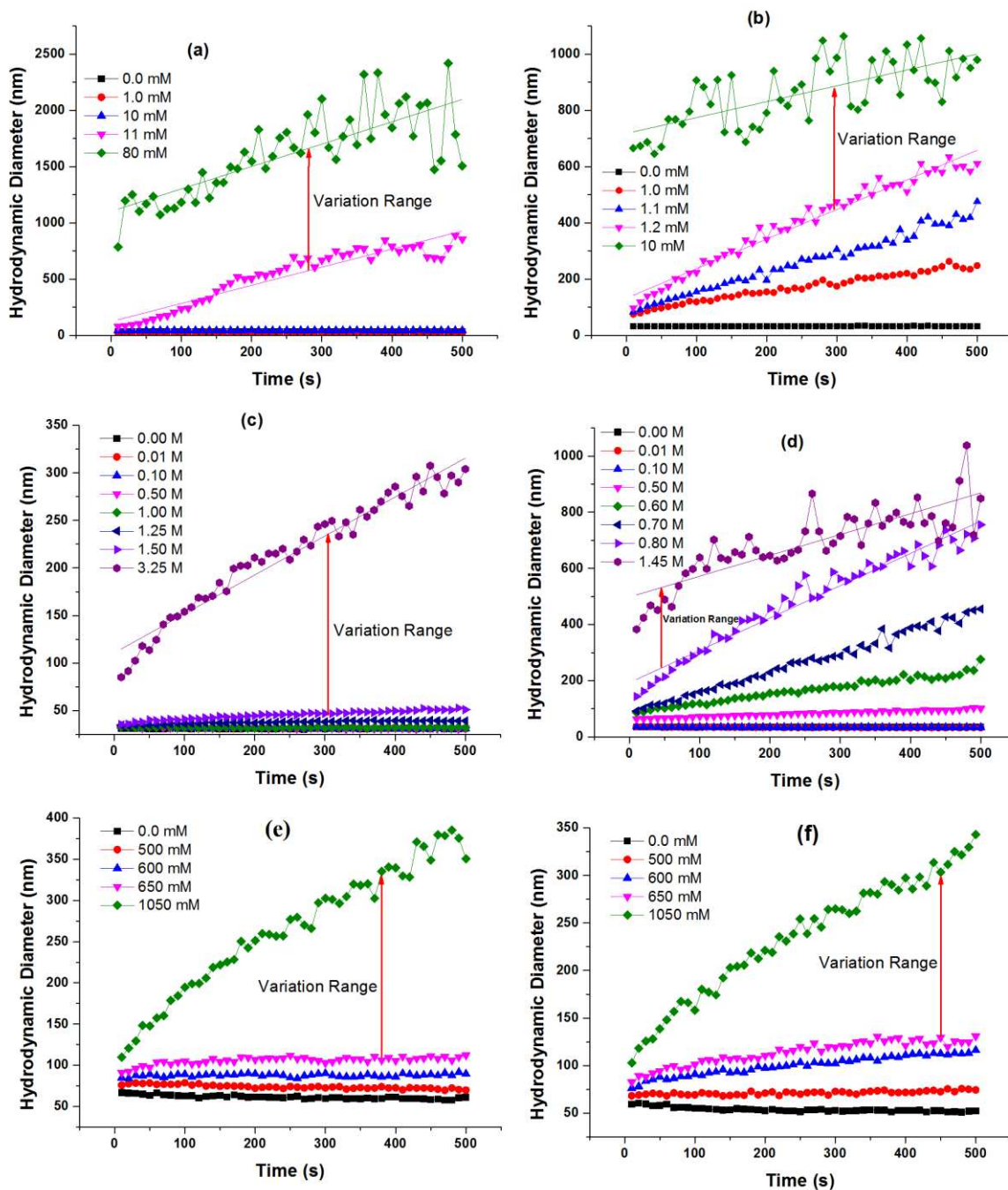


182

183 Figure 3: Effect of surfactants and pH on hydrodynamic diameter and zeta potential of 20ppm
 184 spherical anatase TiO_2 NP: a) Size at the start of experiment, b) Zeta potential at the start of
 185 experiment, c) Size after one week, d) Zeta potential after one week, e) Size after two weeks and f)
 186 Zeta potential after two weeks (All measurements were taken at $\text{pH } 6.5 \pm 0.2$ without any electrolyte).

187 A comparison of the zeta potential for 2 weeks (figure 3 b, d and f) showed no significant difference
 188 for all surfactants at all pH values except sodium citrate, which showed a slight increase in value at
 189 pH 4-7 (figure 3f). Consistency in zeta potential after 2 weeks shows that all sites on the particle
 190 surfaces are occupied by relevant charges which stabilized the hydrodynamic diameter and zeta

191 potential. This is also true for SRFA10 (i.e. 10 ppm SRFA) which was not able to provide enough
 192 negative charges to cover all particles and their surfaces. In comparison, SRFA100 (i.e. 100 ppm
 193 SRFA) provided enough concentration of charges to stabilize the dispersion. Sodium citrate (i.e. 0.3
 194 weight percentage) and SRFA100 were used for below studies.



196 Figure 4: Effect of (a) CaCl_2 on sodium citrate stabilized ellipsoids; (b) CaCl_2 on SRFA stabilized
197 ellipsoids; (c) NaCl on sodium citrate stabilized ellipsoids;(d) NaCl on SRFA stabilized ellipsoids; (e)
198 NaCl on sodium citrate stabilized spherical NP and (f) NaCl on SRFA stabilized spherical NP (NP
199 concentration of 20ppm, SRFA concentration of 100 ppm and $\text{pH}=6.5\pm 0.2$)

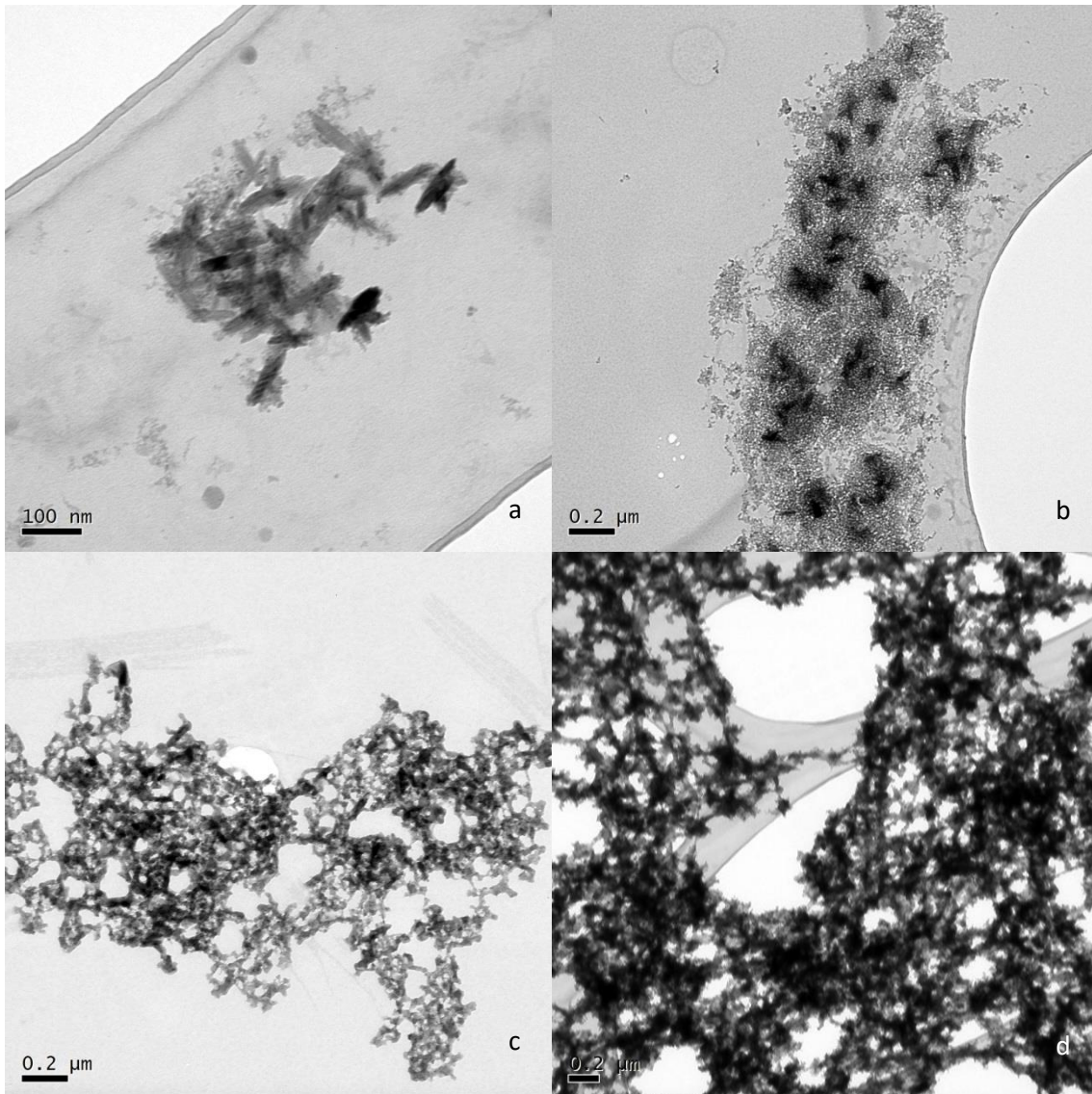
200 **Impact of ionic strength on the aggregation of TiO_2 NP**

201 The aggregation of nanoparticles showed a strong dependency on the ionic strength of the
202 electrolyte dispersion. It was noted that with the addition of electrolytes, there was very slight change
203 in pH values, i.e. ± 0.2 , and the variation pH of the final dispersion was remained in the range of 6.5-
204 7.0.

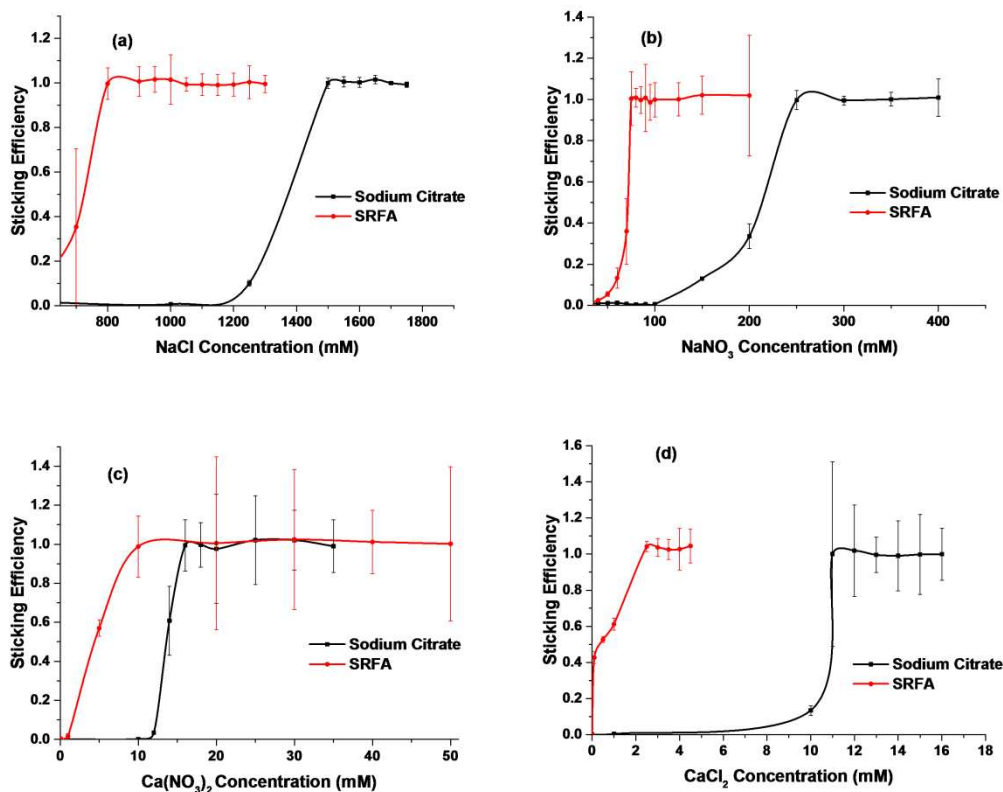
205 Impact on rutile ellipsoids

206 When treated with different salts, the rutile ellipsoids readily formed aggregates within 10 seconds
207 of salt addition. During the first 10 seconds $\text{Ca}(\text{NO}_3)_2$ gave an average aggregate diameter of
208 585.4 ± 22.9 nm and 530.3 ± 31.7 nm for sodium citrate and SRFA stabilized rutile ellipsoids
209 respectively. Whereas the aggregates were slightly smaller in the case of CaCl_2 i.e. 531.9 ± 5.1 nm and
210 366.1 ± 4.9 nm for sodium citrate and SRFA stabilized ones respectively. For the sodium citrate
211 stabilized ellipsoids treated with NaCl and NaNO_3 there was a very slight change in the initial
212 hydrodynamic diameter with average diameter of 65.3 ± 2.1 nm and 59.8 ± 0.2 nm respectively. SRFA
213 stabilized aggregates showed an average diameter of 247.7 ± 20.2 nm and 190.8 ± 2.9 nm for NaCl and
214 NaNO_3 respectively (Figure 4). Clearly the initial aggregate sizes in divalent salts (Figure 4 a and b)
215 were larger than monovalent salts (Figure 4 c and d). Sodium citrate stabilized NP aggregation was
216 entirely different than SRFA stabilized as CCC point reached quickly while in case of SRFA
217 stabilized the CCC point reached slowly with addition of salts. Moreover the salt concentration
218 variation range was much larger in case of sodium citrate stabilized NP as compared to SRFA
219 stabilized (Figure 4). This is consistent with some previous reports showing quick formation of NP
220 aggregates for different NP^{21, 40, 41}. For example French et. al.²¹ reported that 4–5 nm TiO_2 NP quickly
221 formed stable aggregates of hydrodynamic diameter of 50–60 nm in presence of 0.0045 M NaCl at

222 pH of 4.5. At same pH value and 0.0165 M NaCl ionic strength, micron-sized aggregates were formed
223 within 15 minutes. This time was decreased to 5 minutes at pH values 5.8–8.2 even at low NaCl ionic
224 strength of 0.0084–0.0099 M. This aggregation time was 10 fold greater in an aqueous dispersion of
225 0.0128 M CaCl₂ and pH of 4.8. In another study Chen et. al.³⁶ studied that the divalent salts CaCl₂ and
226 MgCl₂ gave much higher aggregate growth rate of alginate-coated hematite NP than that of
227 monovalent NaCl. This process of aggregation was controlled by the thermodynamics where NP
228 reduced their energies to form large aggregates. Figure 5 shows selected TEM micrographs of all salts
229 used, which illustrates that there is an aggregate size and structural difference in the presence of
230 monovalent (Figure 5 a&b) and divalent (Figure5 c&d) salts.



233 Figure 5: TEM images of aggregate formation behaviour and fractal dimensions of a) NaCl
 234 (1380mM) b) NaNO₃ (238mM) c) Ca(NO₃)₂ (16mM) d) CaCl₂ (10.7mM) on 20ppm sodium citrate
 235 stabilized TiO₂ ellipsoids (IS for these images corresponds to the CCC values represented in Table 1;
 236 pH=6.5±0.2).



237
 238 Figure 6: Sticking efficiency of sodium citrate and SRFA stabilized ellipsoids titania (20ppm) against
 239 a) NaCl b) NaNO₃ c) Ca(NO₃)₂ d) CaCl₂ (pH=6.5±0.2).

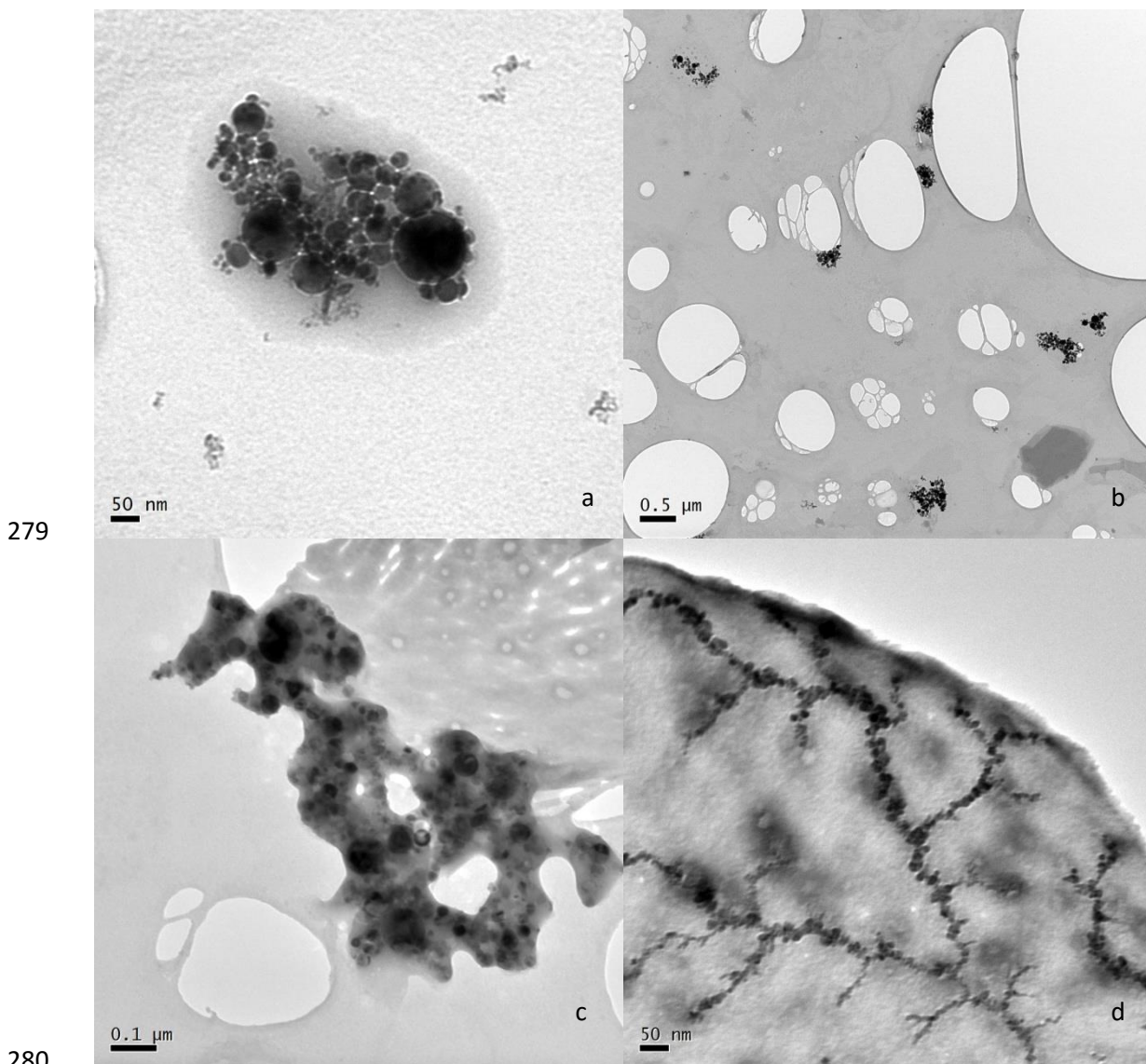
240 As shown in Figure 6, there is a general trend of destabilizing NP with the increase of salt
 241 concentration. For mono valence salts, the sodium citrate stabilized ellipsoids showed better stability
 242 with a critical coagulation concentration of 1380 ± 10 mM NaCl (Figure 6a). While for SRFA, the
 243 CCC was reduced to 790 mM NaCl (figure 6a). Similarly NaNO₃ gave the CCC of 238 mM for
 244 sodium citrate stabilized NP, which was much higher than SRFA stabilized NP with the CCC of 72
 245 mM (Figure 6b).

246 The divalent ion behaved quite different from the monovalent salts. In the presence of $\text{Ca}(\text{NO}_3)_2$, the
247 CCC was 16 mM (Figure 6c) for sodium citrate stabilized ellipsoids, which was reduced to 8.9 mM
248 for SRFA stabilized NP. In the presence of CaCl_2 , the CCC was observed as 10.7 mM and 4.2 mM for
249 sodium citrate stabilized ellipsoids (figure 6d) and SRFA stabilized NP. While these results were
250 similar in the general trend with the monovalent salts, the CCC values were much smaller, indicating
251 that TiO_2 NP were more prone to be destabilized by the presence of divalent salts. The sticking
252 efficiencies in the presence of monovalent salts showed a minimal rise as compared to divalent salts.
253 It might be due to the degree of Debye-Hückel charge screening in monovalent salts is relatively less
254 than divalent salts. This difference in CCCs is mainly because that Ca^{2+} ions have high efficiency to
255 form complexes with citrate and fulvic acid⁴². It was noted that the CCCs of both SRFA and sodium
256 citrate stabilized ellipsoids in the presence of divalent ions are much lower than the CCCs of
257 monovalent salts. It is well documented that the dominant interacting mechanism is the interaction of
258 Ca^{+2} ions with carboxyl groups in citrate, and the bridging complex with fulvic acid and humics
259 characteristics are important from complex formation^{36, 43-46}. Both of these reactions basically
260 neutralized the stabilization effect hence causing quick destabilization of NP. Moreover this inequality
261 of CCCs is most likely due to the lower tendency of monovalent cations to form complexes as
262 compared to higher propensity of divalent cations, hence having higher CCC values.

263 When concentration of mono or divalent salt is increased gradually, the amount of charge screening
264 increases, allowing an increase in aggregation kinetics. This type of aggregation is called reaction-
265 limited aggregation. When the concentration of mono or divalent salts is very high, the charge of
266 stabilized NP is fully screened eliminating the energy barrier between NP. Such an aggregation is
267 called diffusion-limited aggregation where the aggregation kinetics approached to the maximum and
268 is independent of the salt concentration. The CCC is actually the intersection of the cross-over point
269 between both reaction and diffusion limited aggregation points. At high concentrations of mono and
270 divalent salts, the overall charge of TiO_2 NP is totally screened and the energy barrier between NP is
271 eliminated.

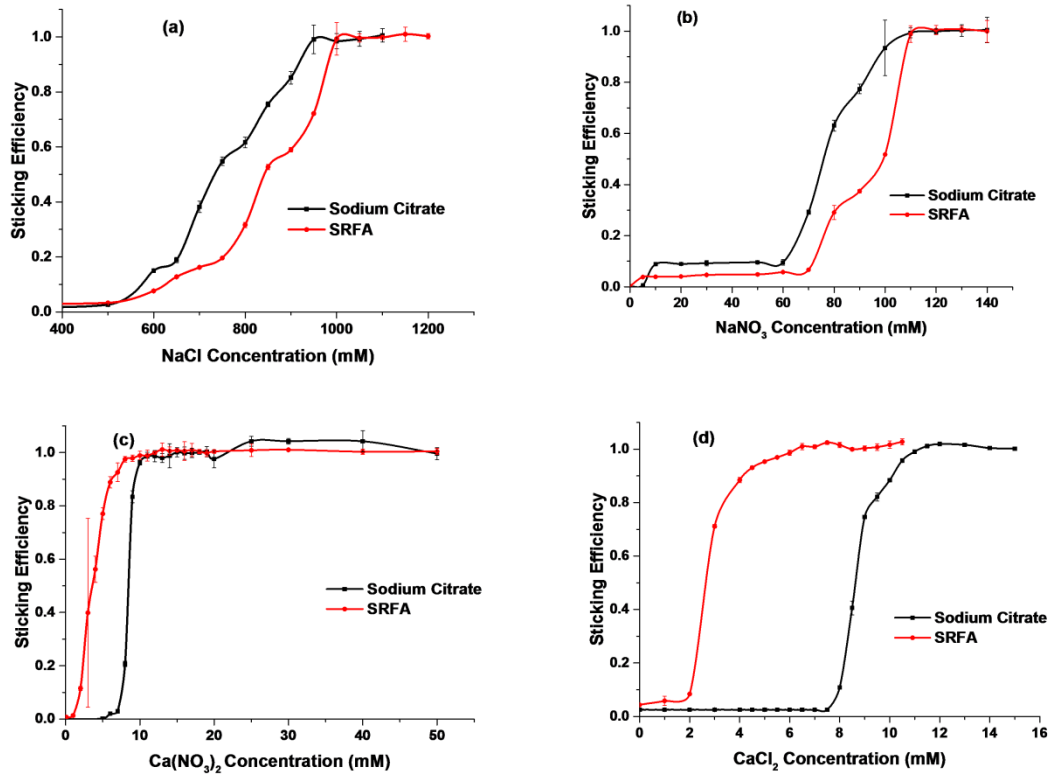
272 **Impact on anatase spherical NP**

273 The overall roundness of NP can be determined with a parameter called shape factor (α) which is
274 defined as “the ratio of the surface area of a nonspherical nanoparticle (S^0) to that of a spherical
275 nanoparticle (S), where both of the nanoparticle have identical volume, i.e. $\alpha = S^0/S^{4/3}$. Due to many
276 fluctuations in the aggregation behaviour of rutile ellipsoids as described above, round anatase NP
277 with a shape factor of 0.9 or above were selected. The aggregation behaviour of round particles was
278 different from the ellipsoids (Figure 5 and 7).



281 Figure 7: TEM images of aggregate formation behaviour and fractal dimensions of a) NaCl (900mM)
282 b) NaNO₃ (90mM) c) Ca(NO₃)₂ (9.8mM) d) CaCl₂ (10.2mM) on 20ppm sodium citrate stabilized

283 spherical TiO₂ NP. (IS for these images corresponds to the CCC values represented in table 1;
284 pH=6.5±0.2).



285
286 Figure 8: Sticking efficiency of sodium citrate and SRFA stabilized spherical anatase NP (20 ppm)
287 against a) NaCl b) NaNO₃ c) Ca(NO₃)₂ d) CaCl₂ (pH=6.5±0.2)

288 For spherical TiO₂ NP, the results obtained from three measurements were more consistent, as
289 shown by the small standard deviation values in Figure 8. In the presence of divalent salts, the
290 agglomeration results were similar between spherical and ellipsoid TiO₂, where the CCC values were
291 consistently lower for SRFA stabilized dispersions. However for monovalent salt, the CCC has
292 shown smaller values for sodium citrate stabilized dispersions. For instance, the CCCs were 900 mM
293 and 1025 mM respectively for sodium citrate and SRFA stabilized NP in the presence of NaCl.
294 Similarly in the presence of NaNO₃, the CCC values were 90 mM and 115 mM respectively for
295 sodium citrate and SRFA stabilized NP. A summary of the CCC values is provided in Table 1.

296

297 Table 1 Comparison of TiO₂ ellipsoids and spherical TiO₂ NP CCC values (20 ppm NP concentration)

Salt	Stabilizing agent	CCC (mM) ellipsoids	CCC (mM) spherical NP
NaCl	0.01% SRFA	790	1000
NaCl	0.3% Sod. citrate	1380	900
NaNO ₃	0.01% SRFA	72	110
NaNO ₃	0.3% Sod. citrate	238	90
Ca(NO ₃) ₂	0.01% SRFA	8.9	6.2
Ca(NO ₃) ₂	0.3% Sod. citrate	16	9.8
CaCl ₂	0.01% SRFA	4.2	3.9
CaCl ₂	0.3% Sod. citrate	10.7	10.2

298

299 DISCUSSIONS

300 Aggregation of TiO₂ nanomaterials in the presence of Sodium Chloride

301 The aggregation kinetics of TiO₂ NP in NaCl varied with the type of stabilizing agents. Results for
 302 sodium citrate stabilized titania ellipsoids reproduced in Fig 6a were in accordance with DLVO theory
 303 and gave a CCC of 1380 mM NaCl. This result was beyond the expectations but sodium citrate
 304 stabilized spheres also resulted in a CCC value of 790mM (Fig 6a & Table 1). However, the CCC for
 305 SRFA stabilized spherical NP was a bit higher than the CCC values ellipsoids (Fig 6a, 8a & Table 1).

306 There was an obvious difference in sticking efficiencies and the initial particle size of both types of
 307 SRFA stabilized nanomaterials. A change in NaCl concentration showed an obvious difference in the
 308 aggregates structure with a change of particle morphology (fig 6a, 8a & table 1). This observation is
 309 consistent with the observation made by Huynh et. al (2011) while treating spherical citrate-coated Ag
 310 NP with NaCl concentrations⁴⁴. The current results show that sodium citrate stabilized ellipsoids have
 311 more stability against NaCl as compared to SRFA, while sodium citrate stabilized spherical NP
 312 showed lower CCC values compared to SRFA.

313 The stability and aggregation differences for two different shapes, i.e. spherical and ellipsoids are
314 mainly because of arrangement of stabilizing ions and polymer chains. These packing arrangements in
315 reaction and diffusion limited regimes for ellipsoids and spherical NP curvatures are shape specific
316 and give distinctiveness to each type⁴⁸.

317 In current research, the spherical TiO₂ NP have higher curvature as compared to the TiO₂ ellipsoids.
318 This detailed surface information alter the physical packing of the stabilizing agent resulting a more
319 compact layer of stabilizing agent for spherical NP as compared to more extended layer for the
320 ellipsoids. This arrangement of the stabilizing agent resulted in higher electrosteric interactions on the
321 curvatures of ellipsoids, giving them enhanced stability at reaction limited regime. While at diffusion
322 limited regime, the ellipsoids gave more stabilization because of higher physical packing with larger
323 amounts of cations.

324 Nanorods are proved to have higher physical packing hindrances as compared to small packing
325 density in nanospheres⁴⁹. Thus electrosteric interactions at reaction limited regime and physical
326 hindrances arrangements of the stabilizing agent in diffusion limited regime are considered as
327 proposed mechanism for the morphological effect of nanoparticles on aggregation. So it is well
328 understood that this behaviour of ellipsoids is due to steric interactions for the particles having larger
329 aspect ratio. In one study on colloidal haematite, Boxall et al.⁵⁰ distinguished that dicarboxylic organic
330 acids provided steric effects and promoted aggregation.

331 It is well documented in the literature that the nanoparticles stabilized with carboxylic acids were
332 more homogenized and possess more negative surface charge as compared to those synthesized in
333 water alone⁵¹. So sodium citrate could influence more on the electrosteric effect in case of ellipsoids
334 with higher aspect ratios than spherical NP. In both cases of SRFA and sodium citrate, all NP
335 contained net negative charges which are being repelled by the negative counter ions on the
336 nanoparticles surface. This repulsion is more in case of ellipsoids due to increased surface area as
337 compared to counter ion effect of round NP.

338 Ellipsoids stabilized with SRFA exhibited aggregation behaviour quite similar to that for SRFA
339 stabilized spherical NP (Figure 6a, 8a & Table 1). There was no obvious increase in the CCC both for
340 ellipsoids and spherical NP stabilized with SRFA. SRFA may enhance particle stability by promoting
341 electrosteric repulsion. The initial particle size of nanomaterial did not increase until the concentration
342 of NaCl reached 500 mM for SRFA and 1250 mM for sodium citrate stabilized ellipsoids (Figure 4 c
343 and d). In comparison, this growth started from 500 mM of NaCl for sodium citrate and SRFA
344 stabilized spherical NP (Figure 4 e&f). These results clearly suggest the influence of aspect ratio,
345 which enhanced stability of NP under same dispersion conditions. It is well documented that synthetic
346 or natural stabilizing agents restrain electron transfer reactions because they reduce accessibility of the
347 available surface area to stop reactions and increase stability^{23, 52, 53}.

348 Another reason for the stability of SRFA stabilized NP is the hydrophobicity of FA⁵⁴. As per IHSS
349 proton-binding study of the functional group charge densities, the phenol-carboxylic ratio of FA is
350 0.25 with a molecular weight of 500-2000 g/mol⁵⁴. In this study NP stabilized with SRFA due to its
351 greater hydrophobicity⁵⁵ and stronger steric repulsion²³; resisted more to the addition of salts
352 irrespective of the shape. TiO₂ ellipsoids with SRFA provided greater stability as compared to
353 spherical NP under similar conditions.

354 Erhayem and Sohn⁵⁶ studied that adsorption of SRFA to the nano-TiO₂ surface was dependent on
355 ionic strength regardless of the pH of media. With an increase in ionic strength, the SRFA would
356 become more twisted and compact. This twisting might give some more nanoparticles surface area to
357 be occupied by the SRFA giving a secondary stability. Therefore the amount of adsorption of SRFA
358 on the surface of TiO₂ NP is highly dependent on the ionic strength. This twisting of the SRFA
359 explains the higher stability of ellipsoids as compared to spherical NP because of more surface area of
360 ellipsoids. At acidic pH, the TiO₂ surface has positive charges so cations give a bridging effect
361 between positively-charged TiO₂ surface and negatively-charged SRFA, again imparting a secondary
362 stability. Although this imparted stability loses its magnitude with increasing ionic strength, it might
363 be a factor for the increased stability of ellipsoids due to increased surface area.

364 **Aggregation of TiO₂ nanomaterials in the presence of Sodium Nitrate**

365 The sodium citrate and SRFA stabilized titania nanomaterials behaved like NaCl aggregation when
366 treated with NaNO₃. The CCC for citrate-coated nanoparticles in NaNO₃ was 72 mM (Figure 6b &
367 Table 1) for SRFA stabilized ellipsoids which increased to 110mM for spherical NP (Figure 6b &
368 Table 1). There was a drop in CCC, from a value of 238mM for titania ellipsoids (Figure 6b & Table
369 1) to 90mM NaNO₃ (Figure 8b & Table 1) which was similar to the value measured in case of NaCl.
370 These CCC values are far less than NaCl CCC values although it was thought that both salts are
371 mono-valent. As compared to NaCl, sodium citrate provided a degree of steric stability to the
372 ellipsoids. The starting hydrodynamic size of the sodium citrate stabilized nanomaterials in NaNO₃,
373 just like in NaCl, followed a decreasing trend with increasing electrolyte concentration initially (fig 6b
374 & 8b). It was noted that the aggregate sizes were higher in high concentrations of NaNO₃ than in
375 similar concentrations of NaCl, suggesting the effect of stabilizing agents was enhanced in NaNO₃
376 than in NaCl. Moreover, in the presence of NO₃⁻, an open fractal structure was observed for the
377 aggregated NP (Figure 7 b&d); however Cl⁻ gave closed fractal structures (Figure 7 a&c), which are
378 the characteristics of aggregation under unfavorable circumstances. So NO₃⁻ always gave larger and
379 open structures in all the cases and Cl⁻ gave smaller aggregate structures (Figure 5).

380 It was observed that CCC was different for differently stabilized NP and for NaCl or NaNO₃, which
381 obviously suggests that the electrolyte anion have somehow very important role and it was not a
382 ligand only. The role of anion was further confirmed by obvious differences in the aggregation of
383 sodium citrate stabilized NP in NaCl and NaNO₃. The difference in the CCC and aggregation
384 behaviour was not dependent on ion size, because the hydrated radius of Cl⁻ at 3.32 Å and NO₃⁻ at
385 3.35 Å⁵⁷ are quite close and might not be able to give much difference in behaviour. It might be NO₃⁻
386 which made the gel like complexes with SRFA and sodium citrate. CCC values of two types of anions
387 reveal that anion effect depends on the type of electrolyte. Stability of TiO₂ ellipsoids and spherical
388 NP is affected at very low concentrations of Cl⁻ and NO₃⁻ for divalent salts while huge amount of Cl⁻
389 was required to destabilize both types of NP in case of NaCl. As Ca⁺ always form a gel-like
390 aggregates³⁶ and NO₃ forms open fractal branched structures, Ca(NO₃)₂ make larger aggregates as

391 compared to monovalent salts or divalent Ca^+ with Cl^- . This is well confirmed while observing the
392 sticking efficiencies where monovalent electrolytes gave more stability with higher CCC values. The
393 combined effect of the gel-like aggregates effect of Ca^+ with the open fractal structures of NO_3^- is the
394 possible reason of larger aggregate size and lower CCC values for $\text{Ca}(\text{NO}_3)_2$. The aggregation state in
395 all cases is related to the overall surface area, adsorption of anion and the sorbate surface exposure.
396 CCC results showed that the greater the attraction of anions by TiO_2 surface, the lower is the stability
397 and vice versa.

398 **Aggregation of TiO_2 nanomaterials in the presence of Calcium Nitrate**

399 $\text{Ca}(\text{NO}_3)_2$ showed aggregation behaviour which was quite in line with NaNO_3 (Table 1). No
400 changes were observed between CCC values of both types of NP but these CCC values are far less
401 than NaNO_3 CCC value, which was attributed to Ca^{+2} because of its quick screen of surface charge by
402 divalent ions. This enhancement in aggregation might be due to the compression of the electrical
403 diffused double layer on TiO_2 NP surface as a result of chelation between NP surface and Ca^{2+} . The
404 results show that the CCC for the SRFA stabilized TiO_2 NP (either ellipsoids or spherical) was at least
405 an order of magnitude higher than sodium citrate coated NP.

406 Both type of TiO_2 NP either coated with SRFA or sodium citrate had negative zeta potential values.
407 With the addition of divalent calcium cations, the zeta potential of stabilized NP decreased. It is well
408 documented in literature that Ca^{2+} forms a complex with organic matter stabilized hematite NP, which
409 neutralized the negative surface charge of the NP³⁶. In the presence of divalent Ca^{2+} , same mechanism
410 governs the destabilization of both types of NP. SRFA imparted the negative charge on the surface of
411 both types of TiO_2 NP. These imparted negative charges made complex with Ca^{2+} to destabilize the
412 NP dispersion even with little amounts of the divalent salt.

413 **Aggregation of TiO_2 nanomaterials in the presence of Calcium Chloride**

414 The aggregation behaviour observed in CaCl_2 was similar to that observed in NaCl but the NP
415 started to aggregate at a lower concentration of CaCl_2 . The stability of the SRFA stabilized
416 nanomaterials in CaCl_2 was obviously different from that in NaCl , as divalent cations quickly changed

417 the aggregation stage. The ellipsoids either stabilized by sodium citrate or SRFA showed a better
418 magnitude of stability as compared to spherical NP mainly due to the greater surface area. This clearly
419 illustrates the effect of shape on the stability of NP. The high charge screening efficiency of Ca^{+2} ions
420 for the nanomaterials could be the possible aggregation mechanisms along with the specific
421 interaction of nanomaterials, Ca^{+2} ions and stabilizing agents⁵⁸.

422 Huynh and Chen⁴⁴ considered the interparticle bridging of NP by interaction of humic acid and Ca^{2+}
423 ions as the main reason of aggregation. They emphasized that polymer coated NP had more stability
424 as compared to citrate coated NP in the presence of monovalent and divalent ions. This is more likely
425 because of the electrosteric stability induced by large chain polymers. The sticking of SRFA
426 molecules imparted additional stability to the NP in the presence of low concentrations of ions. But
427 when the concentration was high, the intermolecular bridging induced by SRFA gave enhanced
428 aggregation.

429 **CONCLUSIONS**

430 This study showed that the surfactant, ionic strength and morphology of TiO_2 NP affected the
431 aggregation kinetics significantly. Five surfactants were investigated influencing the aggregation
432 process but sodium citrate and SRFA were the most effective stabilizing agents. NP morphology has
433 influenced the sticking efficiency and crystal structure, which altered the aggregation kinetics TiO_2
434 ellipsoids proved more resistant to aggregation than spherical NP against different Ca^{+2} and Na^+ salts
435 at similar concentrations. Salt concentrations changed the sticking efficiency between individual NP
436 and NP-substrate surfaces. It is considered that the aggregation kinetics is due to Ca^{+2} and Na^+ cations
437 but CO_3^- and Cl^- anions may also have their impacts, which will be studied in future work.

438 **ENVIRONMENTAL IMPLICATIONS**

439 SRFA stabilized NP are relatively more stable than sodium citrate stabilized NP, mainly due to the
440 electrosteric repulsion by the SRFA molecules. Since the CCC values for both types of NP are greater
441 than typical environmental related concentrations of mono and divalent salt concentrations, it is

442 presumed that these NP are highly mobile in natural environments. Moreover natural environments
443 have fulvic and humic acids in abundance which naturally increase the stability of these NP hence
444 increasing their mobility. This work acts as a benchmark study to understand the ultimate fate of
445 engineered nanoparticles in the environment. Clearly due to the complexities in real soil matrix,
446 which would have different complex nature of ions and natural organic matters, understanding the real
447 time fate of engineered nanoparticles is still a big challenge. Clearly there is still a strong need of
448 further studies to establish the influence of other environmental constituents like natural organic
449 matters, humic acids and different metals on the aggregation kinetics of titania NP. In addition, further
450 research work is needed to assess the effect of different sizes and phase contents on NP stability,
451 aggregation kinetics and mobility.

452

453 **AUTHOR INFORMATION**

454 ***Corresponding Authors**

455 Phone: +44 113 343 1299, Email: d.wen@leeds.ac.uk

456 Phone: +44 113 343 2350, Email: g.raza@leeds.ac.uk

457 Acknowledgement

458 This work was supported by European Research Council Consolidator Grant (Grant
459 number: 648375).

460 **References**

- 461 (1. Rao, C. N. R.; Müller, A.; Cheetham, A. K., *The chemistry of*
462 *nanomaterials*. Wiley. com: 2006; Vol. 1.
- 463 2. Gottschalk, F.; Sonderer, T.; Scholz, R. W.; Nowack, B.,
464 Modeled environmental concentrations of engineered nanomaterials
465 (TiO₂, ZnO, Ag, CNT, fullerenes) for different regions.
466 *Environmental Science & Technology* **2009**, *43*, (24), 9216-9222.
- 467 3. Tsuji, J. S.; Maynard, A. D.; Howard, P. C.; James, J. T.;
468 Lam, C.-w.; Warheit, D. B.; Santamaria, A. B., Research Strategies
469 for Safety Evaluation of Nanomaterials, Part IV: Risk Assessment of
470 Nanoparticles. *Toxicological Sciences* **2006**, *89*, (1), 42-50.
- 471 4. Grass, R. N.; Tsantilis, S.; Pratsinis, S. E., Design of high-
472 temperature, gas-phase synthesis of hard or soft TiO₂ agglomerates.
473 *AIChE Journal* **2006**, *52*, (4), 1318-1325.
- 474 5. Mandzy, N.; Grulke, E.; Druffel, T., Breakage of TiO₂
475 agglomerates in electrostatically stabilized aqueous dispersions.
476 *Powder Technology* **2005**, *160*, (2), 121-126.
- 477 6. Kretzschmar, R.; Schäfer, T., Metal Retention and Transport on
478 Colloidal Particles in the Environment. *Elements* **2005**, *1*, (4), 205-
479 210.
- 480 7. Kataoka, S.; Gurau, M. C.; Albertorio, F.; Holden, M. A.; Lim,
481 S.-M.; Yang, R. D.; Cremer, P. S., Investigation of Water Structure
482 at the TiO₂/Aqueous Interface. *Langmuir* **2004**, *20*, (5), 1662-1666.
- 483 8. Klaine, S. J.; Alvarez, P. J. J.; Batley, G. E.; Fernandes, T.
484 F.; Handy, R. D.; Lyon, D. Y.; Mahendra, S.; McLaughlin, M. J.;
485 Lead, J. R., Nanomaterials in the environment: Behavior, fate,
486 bioavailability, and effects. *Environmental Toxicology and Chemistry*
487 **2008**, *27*, (9), 1825-1851.
- 488 9. Chen, J.; Xiu, Z.; Lowry, G. V.; Alvarez, P. J. J., Effect of
489 natural organic matter on toxicity and reactivity of nano-scale
490 zero-valent iron. *Water Research* **2011**, *45*, (5), 1995-2001.
- 491 10. Edgington, A. J.; Roberts, A. P.; Taylor, L. M.; Alloy, M. M.;
492 Reppert, J.; Rao, A. M.; Mao, J.; Klaine, S. J., The influence of
493 natural organic matter on the toxicity of multiwalled carbon
494 nanotubes. *Environmental Toxicology and Chemistry* **2010**, *29*, (11),
495 2511-2518.
- 496 11. Wang, C.-y.; Bahnemann, D. W.; Dohrmann, J. K., A novel
497 preparation of iron-doped TiO₂ nanoparticles with enhanced
498 photocatalytic activity. *Chemical Communications* **2000**, (16), 1539-
499 1540.
- 500 12. Mylon, S. E.; Chen, K. L.; Elimelech, M., Influence of Natural
501 Organic Matter and Ionic Composition on the Kinetics and Structure
502 of Hematite Colloid Aggregation: Implications to Iron Depletion in
503 Estuaries. *Langmuir* **2004**, *20*, (21), 9000-9006.

- 504 13. Dunnivant, F. M.; Schwarzenbach, R. P.; Macalady, D. L.,
505 Reduction of substituted nitrobenzenes in aqueous solutions
506 containing natural organic matter. *Environmental Science &*
507 *Technology* **1992**, *26*, (11), 2133-2141.
- 508 14. Navarro, E.; Baun, A.; Behra, R.; Hartmann, N.; Filser, J.;
509 Miao, A.-J.; Quigg, A.; Santschi, P.; Sigg, L., Environmental
510 behavior and ecotoxicity of engineered nanoparticles to algae,
511 plants, and fungi. *Ecotoxicology* **2008**, *17*, (5), 372-386.
- 512 15. Zhang, W., Nanoparticle aggregation: principles and modeling.
513 In *Nanomaterial*, Springer: 2014; pp 19-43.
- 514 16. Allen, L. H.; Matijević, E., Stability of colloidal silica: I.
515 Effect of simple electrolytes. *Journal of Colloid and Interface*
516 *Science* **1969**, *31*, (3), 287-296.
- 517 17. Pfeiffer, C.; Rehbock, C.; Hühn, D.; Carrillo-Carrion, C.; de
518 Aberasturi, D. J.; Merk, V.; Barcikowski, S.; Parak, W. J.,
519 Interaction of colloidal nanoparticles with their local environment:
520 the (ionic) nanoenvironment around nanoparticles is different from
521 bulk and determines the physico-chemical properties of the
522 nanoparticles. *Journal of the Royal Society Interface* **2014**, *11*,
523 (96), 20130931.
- 524 18. Wang, J.; Mishra, A. K.; Zhao, Q.; Huang, L., Size effect on
525 thermal stability of nanocrystalline anatase TiO₂. *Journal of*
526 *Physics D: Applied Physics* **2013**, *46*, (25), 255303.
- 527 19. Zhang, H.; Gilbert, B.; Huang, F.; Banfield, J. F., Water-
528 driven structure transformation in nanoparticles at room
529 temperature. *Nature* **2003**, *424*, (6952), 1025-1029.
- 530 20. Dunphy Guzman, K. A.; Finnegan, M. P.; Banfield, J. F.,
531 Influence of Surface Potential on Aggregation and Transport of
532 Titania Nanoparticles. *Environmental Science & Technology* **2006**, *40*,
533 (24), 7688-7693.
- 534 21. French, R. A.; Jacobson, A. R.; Kim, B.; Isley, S. L.; Penn,
535 R. L.; Baveye, P. C., Influence of Ionic Strength, pH, and Cation
536 Valence on Aggregation Kinetics of Titanium Dioxide Nanoparticles.
537 *Environmental Science & Technology* **2009**, *43*, (5), 1354-1359.
- 538 22. Logtenberg, E. H. P.; Stein, H. N., Surface charge and
539 coagulation of aqueous ZnO dispersions. *Journal of Colloid and*
540 *Interface Science* **1986**, *109*, (1), 190-200.
- 541 23. Domingos, R. F.; Tufenkji, N.; Wilkinson, K. J., Aggregation
542 of Titanium Dioxide Nanoparticles: Role of a Fulvic Acid.
543 *Environmental Science & Technology* **2009**, *43*, (5), 1282-1286.
- 544 24. Sun, J.; Guo, L.-H.; Zhang, H.; Zhao, L., UV Irradiation
545 Induced Transformation of TiO₂ Nanoparticles in Water: Aggregation
546 and Photoreactivity. *Environmental Science & Technology* **2014**, *48*,
547 (20), 11962-11968.

- 548 25. Jassby, D.; Farner Budarz, J.; Wiesner, M., Impact of
549 Aggregate Size and Structure on the Photocatalytic Properties of
550 TiO₂ and ZnO Nanoparticles. *Environmental Science & Technology* **2012**,
551 46, (13), 6934-6941.
- 552 26. Gummy, D.; Morais, C.; Bowen, P.; Pulgarin, C.; Giraldo, S.;
553 Hajdu, R.; Kiwi, J., Catalytic activity of commercial of TiO₂
554 powders for the abatement of the bacteria (E. coli) under solar
555 simulated light: Influence of the isoelectric point. *Applied*
556 *Catalysis B: Environmental* **2006**, 63, (1-2), 76-84.
- 557 27. Chowdhury, I.; Cwiertny, D. M.; Walker, S. L., Combined
558 Factors Influencing the Aggregation and Deposition of nano-TiO₂ in
559 the Presence of Humic Acid and Bacteria. *Environmental Science &*
560 *Technology* **2012**, 46, (13), 6968-6976.
- 561 28. Amirkhani, M.; Volden, S.; Zhu, K.; Glomm, W. R.; Nyström, B.,
562 Adsorption of cellulose derivatives on flat gold surfaces and on
563 spherical gold particles. *Journal of Colloid and Interface Science*
564 **2008**, 328, (1), 20-28.
- 565 29. Keller, A. A.; Wang, H.; Zhou, D.; Lenihan, H. S.; Cherr, G.;
566 Cardinale, B. J.; Miller, R.; Ji, Z., Stability and Aggregation of
567 Metal Oxide Nanoparticles in Natural Aqueous Matrices. *Environmental*
568 *Science & Technology* **2010**, 44, (6), 1962-1967.
- 569 30. Thio, B. J. R.; Zhou, D.; Keller, A. A., Influence of natural
570 organic matter on the aggregation and deposition of titanium dioxide
571 nanoparticles. *Journal of Hazardous Materials* **2011**, 189, (1-2), 556-
572 563.
- 573 31. Mwaanga, P.; Carraway, E.; Schlautman, M., Preferential
574 sorption of some natural organic matter fractions to titanium
575 dioxide nanoparticles: influence of pH and ionic strength. *Environ*
576 *Monit Assess* **2014**, 186, (12), 8833-8844.
- 577 32. Klitzke, S.; Metreveli, G.; Peters, A.; Schaumann, G. E.;
578 Lang, F., The fate of silver nanoparticles in soil solution –
579 Sorption of solutes and aggregation. *Science of The Total*
580 *Environment*, (0).
- 581 33. Zhou, H.; Zou, Z.; Wu, S.; Ge, F.; Li, Y.; Shi, W., Rapid
582 synthesis of TiO₂ hollow nanostructures with crystallized walls by
583 using CuO as template and microwave heating. *Materials Letters* **2011**,
584 65, (6), 1034-1036.
- 585 34. Zhou, D.; Keller, A. A., Role of morphology in the aggregation
586 kinetics of ZnO nanoparticles. *Water Research* **2010**, 44, (9), 2948-
587 2956.
- 588 35. Yin, H.; Wada, Y.; Kitamura, T.; Sumida, T.; Hasegawa, Y.;
589 Yanagida, S., Novel synthesis of phase-pure nano-particulate anatase
590 and rutile TiO₂ using TiCl₄ aqueous solutions. *Journal of Materials*
591 *Chemistry* **2002**, 12, (2), 378-383.
- 592 36. Chen, K. L.; Mylon, S. E.; Elimelech, M., Aggregation Kinetics
593 of Alginate-Coated Hematite Nanoparticles in Monovalent and Divalent

594 Electrolytes. *Environmental Science & Technology* **2006**, *40*, (5),
595 1516-1523.

596 37. Kim, A. Y.; Berg, J. C., Fractal Aggregation: Scaling of
597 Fractal Dimension with Stability Ratio. *Langmuir* **1999**, *16*, (5),
598 2101-2104.

599 38. Garzella, C.; Comini, E.; Tempesti, E.; Frigeri, C.;
600 Sberveglieri, G., TiO₂ thin films by a novel sol-gel processing for
601 gas sensor applications. *Sensors and Actuators B: Chemical* **2000**, *68*,
602 (1-3), 189-196.

603 39. IUPAC, Compendium of Chemical Terminology Gold Book. **2014**,
604 Dated 2014-02-24, (Version 2.3.3).

605 40. Wang, P.; Keller, A. A., Natural and Engineered Nano and
606 Colloidal Transport: Role of Zeta Potential in Prediction of
607 Particle Deposition. *Langmuir* **2009**, *25*, (12), 6856-6862.

608 41. Sousa, V. S.; Teixeira, M. R., Aggregation kinetics and
609 surface charge of CuO nanoparticles: the influence of pH, ionic
610 strength and humic acids. *Environmental Chemistry* **2013**, *10*, (4),
611 313-322.

612 42. Baalousha, M.; Nur, Y.; Römer, I.; Tejamaya, M.; Lead, J. R.,
613 Effect of monovalent and divalent cations, anions and fulvic acid on
614 aggregation of citrate-coated silver nanoparticles. *Science of The*
615 *Total Environment* **2013**, *454-455*, (0), 119-131.

616 43. Gutierrez, L.; Aubry, C.; Cornejo, M.; Croue, J.-P., Citrate-
617 Coated Silver Nanoparticles Interactions with Effluent Organic
618 Matter: Influence of Capping Agent and Solution Conditions. *Langmuir*
619 **2015**, *31*, (32), 8865-8872.

620 44. Huynh, K. A.; Chen, K. L., Aggregation Kinetics of Citrate and
621 Polyvinylpyrrolidone Coated Silver Nanoparticles in Monovalent and
622 Divalent Electrolyte Solutions. *Environmental science & technology*
623 **2011**, *45*, (13), 5564-5571.

624 45. Kalinichev, A. G.; Iskrenova-Tchoukova, E.; Ahn, W.-Y.; Clark,
625 M. M.; Kirkpatrick, R. J., Effects of Ca²⁺ on supramolecular
626 aggregation of natural organic matter in aqueous solutions: A
627 comparison of molecular modeling approaches. *Geoderma* **2011**, *169*, 27-
628 32.

629 46. Kirishima, A.; Tanaka, K.; Niibori, Y.; Tochiyama, O., Complex
630 formation of calcium with humic acid and polyacrylic acid.
631 *Radiochim. Acta* **2002**, *90*, (9-11), 555-561.

632 47. Qi, W. H.; Wang, M. P.; Liu, Q. H., Shape factor of
633 nonspherical nanoparticles. *Journal of Materials Science* **2005**, *40*,
634 (9-10), 2737-2739.

635 48. Fazio, G.; Ferrighi, L.; Di Valentin, C., Spherical versus
636 Faceted Anatase TiO₂ Nanoparticles: A Model Study of Structural and
637 Electronic Properties. *The Journal of Physical Chemistry C* **2015**,
638 *119*, (35), 20735-20746.

639 49. Rudge, J.; Holness, M.; Smith, G., Quantitative textural
640 analysis of packings of elongate crystals. *Contrib Mineral Petrol*
641 **2008**, *156*, (4), 413-429.

642 50. Boxall, A. B.; Tiede, K.; Chaudhry, Q., Engineered
643 nanomaterials in soils and water: how do they behave and could they
644 pose a risk to human health? *Nanomedicine* **2007**, *2*, (6), 919-927.

645 51. Chang, X.; Vikesland, P. J., Effects of carboxylic acids on
646 nC60 aggregate formation. *Environmental Pollution* **2009**, *157*, (4),
647 1072-1080.

648 52. EU, Commission recommendation of 18 October 2011 on the
649 definition of nanomaterial *Official Journal L* **2011**, *275*, 38-40.

650 53. Li, S.; Sun, W., A comparative study on
651 aggregation/sedimentation of TiO₂ nanoparticles in mono- and binary
652 systems of fulvic acids and Fe(III). *Journal of Hazardous Materials*
653 **2011**, *197*, (0), 70-79.

654 54. Baalousha, M.; Motelica-Heino, M.; Coustumer, P. L.,
655 Conformation and size of humic substances: Effects of major cation
656 concentration and type, pH, salinity, and residence time. *Colloids*
657 *and Surfaces A: Physicochemical and Engineering Aspects* **2006**, *272*,
658 (1-2), 48-55.

659 55. Westerhoff, P.; Mezyk, S. P.; Cooper, W. J.; Minakata, D.,
660 Electron Pulse Radiolysis Determination of Hydroxyl Radical Rate
661 Constants with Suwannee River Fulvic Acid and Other Dissolved
662 Organic Matter Isolates. *Environmental Science & Technology* **2007**,
663 *41*, (13), 4640-4646.

664 56. Erhayem, M.; Sohn, M., Stability studies for titanium dioxide
665 nanoparticles upon adsorption of Suwannee River humic and fulvic
666 acids and natural organic matter. *Science of The Total Environment*
667 **2014**, *468-469*, 249-257.

668 57. Richards, L. A.; Richards, B. S.; Schäfer, A. I., Renewable
669 energy powered membrane technology: Salt and inorganic contaminant
670 removal by nanofiltration/reverse osmosis. *Journal of Membrane*
671 *Science* **2011**, *369*, (1-2), 188-195.

672 58. Konradi, R.; Rühle, J., Interaction of Poly(methacrylic acid)
673 Brushes with Metal Ions: Swelling Properties. *Macromolecules* **2005**,
674 *38*, (10), 4345-4354.

675

676